geoconvention
Calgary • Canada • May 13-17 2019

Fusion of multi-physics data with machine learning independent component analysis (ICA) improves detection of geological features

Hassan H. Hassan & Serguei Goussev
Multiphysics Imaging Technology, Inc.

Summary

Multi-physics data, such as gravity and magnetic, have become one of the oil and gas as well as the mineral industry standard exploration data. Unlike seismic data, aquiring gravity and magnetic data are more time- and cost-effective. Besides, multi-physics data can be acquired from airborne and satellite platforms. This make gravity and magnetic methods more attractive for exploration, because they provide the capability of surveying remote areas that are otherwise impossible or difficult to reach by land, for example the Rocky Mountains. Gravity and magnetic data can also provide crucial information about the subsurface geology and the structure of unexplored areas selected for further detailed seismic surveys. Quite often, airborne gravity and magnetic surveys are flown over the same area and with the same aircraft. Hence, the acquired gravity and magnetic data complement each other in term of their responses to geological targets, with each conribute to the overall output response in proportion to the the density and the magnetic susceptibility values of the target. The detection and the resolving powers of the gravity and the magnetic data are different too. In sedimentary basins, for example, gravity data are more resolving in detecting structural and lithological discontinuities within the sedimentary section of the basin whereas magnetic data are more resolving in detecting structural and lithological discontinuities within the crystalline basement rocks. Accordingly, subsurface geological structures are partially displayed on the gravity image and partially on the magnetic image. Therefore, if we combine the gravity and the magnetic images into a single fused image and use it in our interpretation flow, we would be able to detect geological structures more clearly and more efficiently than if we interpret the gravity and the magnetic images, separately. Fusion combines images from different sources together, to produce a composite image that contains integrated information extracted from the original images. Currently, several techniques are available for image fusion. In this study, a robust technique based on the independent component analysis (ICA) was selected to fuse airborne gravity and magnetic images. ICA is a powerful machine learning statistical technique for performing the blind signal separation (BSS) and it aims at separating overlapping non-Gaussian and statistically independent components that are embedded in the gravity and the magnetic images and fuse them together into a single image. The ICA fusion technique was applied to gravity and magnetic images derived from the same airborne gravity gradiometry survey that was flown over the McFaulds Lake area in Ontario, Canada. To obey Poisson's theorem, we used the image of the first vertical derivative of the Bouguer gravity instead of the image of the Bouguer gravity, as the gravity input in the fusion process. According to Poisson's theorem, the first vertical derivative of the Bouguer gravity anomaly is equivalent to the reduced to the pole total magnetic intensity anomaly. The preliminary results obtained from fusing the gravity and the magnetic images reveal a number of well-defined linear and curvilinear geological structures that are not apparent on the individual input gravity and magnetic images. These linear and curvilinear structures are most likely

represent footprints of folds, faults and fractures intersecting the Precambrian basement and the overlying sedimentary and meta-sedimentary rocks.

Introduction

It is becoming a standard procedure that with every gravity survey, beside gravity data magnetic data are acquired too. Typically, gravity and magnetic data are analyzed and interpreted separately, even though both are complementary to each other in their response to the same geological structure. In order to improve the quality of their interpretation and make it less subjective and more efficient, we made an attempt to combine the gravity and the magnetic images into a single composite image by using fusion. There are a number of image fusion techniques available in the literature for this purpose (Hassan and Peirce, 2008; Goussev *et al*., 2009). However, in this study, we selected a new approach based on the independent component analysis (ICA) to fuse gravity and magnetic images. ICA is a powerful machine learning multivariate statistical technique designed to extract a set of statistically independent components from a mixture of signals (Hyvärinen, 2013). We tested the capability of ICA algorithms to extract independent components (i.e. geological features) from gravity and magnetic images and fuse them into a single image that we belief carry more information than the individual images. The ICA-based fusing algorithm was applied to gravity and magnetic images derived from an airborne gravity gradiometry survey over the McFaulds Lake area (aka, Ring of Fire) in Ontario, Canada. The airborne survey were flown by Fugro (Currently CGG) Airborne Surveys in 2011 using the NW-SE oriented flight lines with 250 m spacing and orthogonal tie lines with 2500 m spacing at nominal terrain clearance of 100 m. The survey was carried out on behalf of the Ontario Geological Survey and Geological Survey of Canada (OGS and GSC, 2011). The study area (Fig. 1) is considered to be one of the most prospective areas for the mineral and, possibly, oil-and-gas exploration. Geologically, the area overlaps the boundary between mostly shallow Archean basement rocks of the Superior Province and overlying Paleozoic sedimentary rocks of the Hudson Platform. It is underlain by the arcuate Neoarchean greenstone belt and sub-vertically dipping mafic and ultramafic intrusions, some of them are layered and crosscut the western portion of the belt (Cranston, 2010). Regional geological mapping shows that the sedimentary rock cover is highly deformed by ultramafic igneous complexes toward the western end of the study area and combined with the Paleozoic sedimentary rocks in its eastern part. Magnetic patterns indicate the presence of complex rock formations composed of the volcanic and sedimentary belts between large expanses of granites and gneisses (Cranston, 2010).

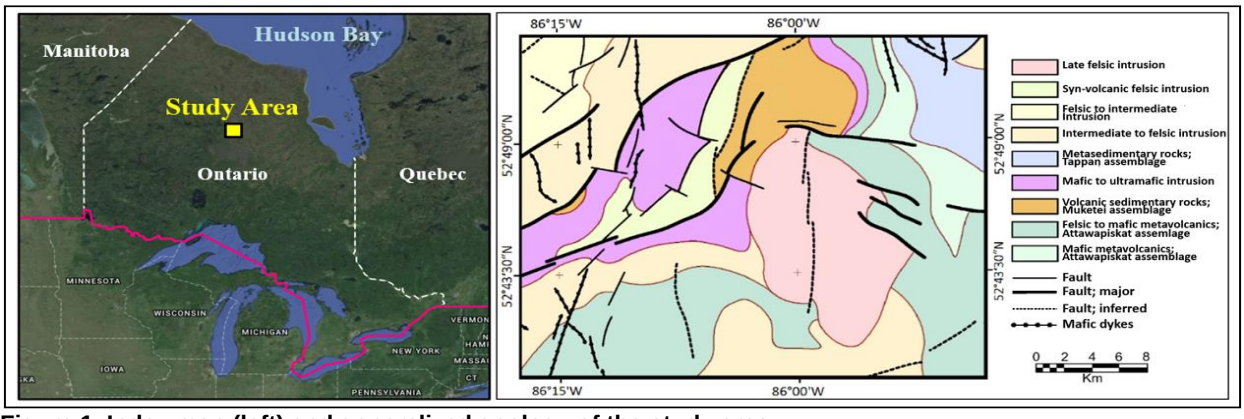

Figure 1. Index map (left) and generalized geology of the study area.

Methodology

The best way to describe the ICA technique is to refer to the 'cocktail party' example illustrated on Figure 2. Here, there are two people speaking simultaneously in a room and their voices ($\mathbf{S_1}$ and $\mathbf{S_2}$) are recorded by two microphones placed at different locations. We assume that the two voices ($\mathbf{S_1}$ and $\mathbf{S_2}$) are non-Gaussian and statistically independent. Their linearly mixed signals are recorded as $\mathbf{X_1}$ and $\mathbf{X_2}$ that can be expressed by the following linear equation:

$$\mathbf{x} = \mathbf{A}\mathbf{s} \qquad (1)$$

Since we are mixing two sources (i.e., gravity and magnetic images), Equation 1 can be expressed as follows:

$$\left\{\begin{matrix} x_1 = a_{11}s_1 + a_{12}s_2 \\ x_1 = a_{11}s_1 + a_{12}s_2 \end{matrix}\right\} \Rightarrow \begin{bmatrix} x_1 \\ x_2 \end{bmatrix} = \begin{bmatrix} a_{11} & a_{12} \\ a_{21} & a_{22} \end{bmatrix} \begin{bmatrix} s_1 \\ s_2 \end{bmatrix} \qquad (2)$$

Both, **A** and **s** are unknown and we try to estimate them by ICA. The parameters ($\mathbf{a_{11}}$, $\mathbf{a_{12}}$, $\mathbf{a_{21}}$, $\mathbf{a_{22}}$) in matrix **A** are related to the distances between the microphones and the two speakers. ICA is aimed to estimate **A** and **s**, and obtain a de-mixing matrix **W**. For simplicity, we assume that the unknown mixing matrix **A** is square. The goal is to recover the original people's voices ($\mathbf{S_1}$ and $\mathbf{S_2}$) when we are only given the observed data (i.e., $\mathbf{X_1}$ and $\mathbf{X_2}$). After estimating the matrix **A**, we can compute its inverse **W** and obtain the independent components $\mathbf{u_1}$ and $\mathbf{u_2}$ (estimated sources) as follows:

$$\mathbf{s} \approx \mathbf{u} = \mathbf{A}^{-1}\mathbf{x} = \mathbf{W}\mathbf{x} \qquad (3)$$

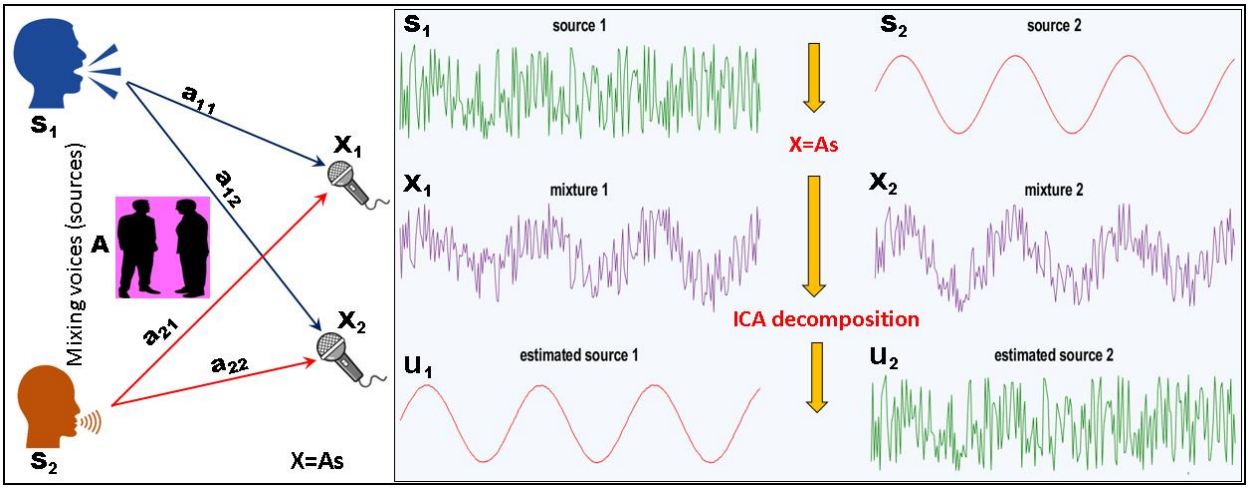

Figure 2. Explanation of ICA technique, using the cocktail party problem as an example.

The workflow that we followed in this study is shown in Figure 3. As illustrated in Figure 3, we used the first vertical derivative of the Bouguer gravity anomaly (Fig. 4b) instead of the original Bouguer gravity anomaly image (Fig. 4a) for the fusion. The reason is to obey the Poisson's theorem in which it states that the first vertical derivative of the Bouguer gravity anomaly is theoretically equivalent to the reduced to the pole total magnetic intensity anomaly.

The linear relationship between the magnetic potential (Φ_M) and the gravity potential (Φ_g) described by the Poisson's theorem is illustrated in the following equation:

$$\phi_M = \frac{1}{G} \cdot \frac{\Delta J}{\Delta_\rho} \cdot \frac{\partial \phi_g}{\partial i} \qquad (4)$$

where **G** is the universal gravity constant (6.670×10^{11} $m^3/kg.s^2$), **ΔJ** is the induced magnetization contrast of the anomalous source, **$\Delta \rho$** is the density contrast of the anomalous source, and ∂/∂**i** is the gradient in the direction of the total magnetization vector.

By differentiating Equation 4 with respect to **z** (i.e., the vertical downward direction), we get Equation 5 in which it shows a close relationship between the reduced to the pole magnetic intensity anomaly (T_z) and the first vertical derivative of the Bouguer gravity anomaly ($\partial g/\partial z$) (Chandler *et al.*,1981):

$$T_z = A + \frac{1}{G} \cdot \frac{\Delta J}{\Delta_\rho} \cdot \frac{\partial g}{\partial z} \qquad (5)$$

where T_z stands for the reduced to pole total magnetic intensity anomaly, $\partial g/\partial z$ is the first vertical derivative of the Bouguer gravity anomaly, and ***A*** is a constant value. Equation 5 is actually represents a least square regression line and it can be rewritten as:

$$T_z = A + S\left(\frac{1}{G} \cdot \frac{\partial g}{\partial z}\right) \qquad (6)$$

where ***A*** is the intercept of the least square regression line between the gravity and the magnetic anomalies, and ***S*** is the slope of the least square regression line and it represents the ratio of the induced magnetization contrast to the density contrast (i.e., $\Delta J/\Delta \rho$).

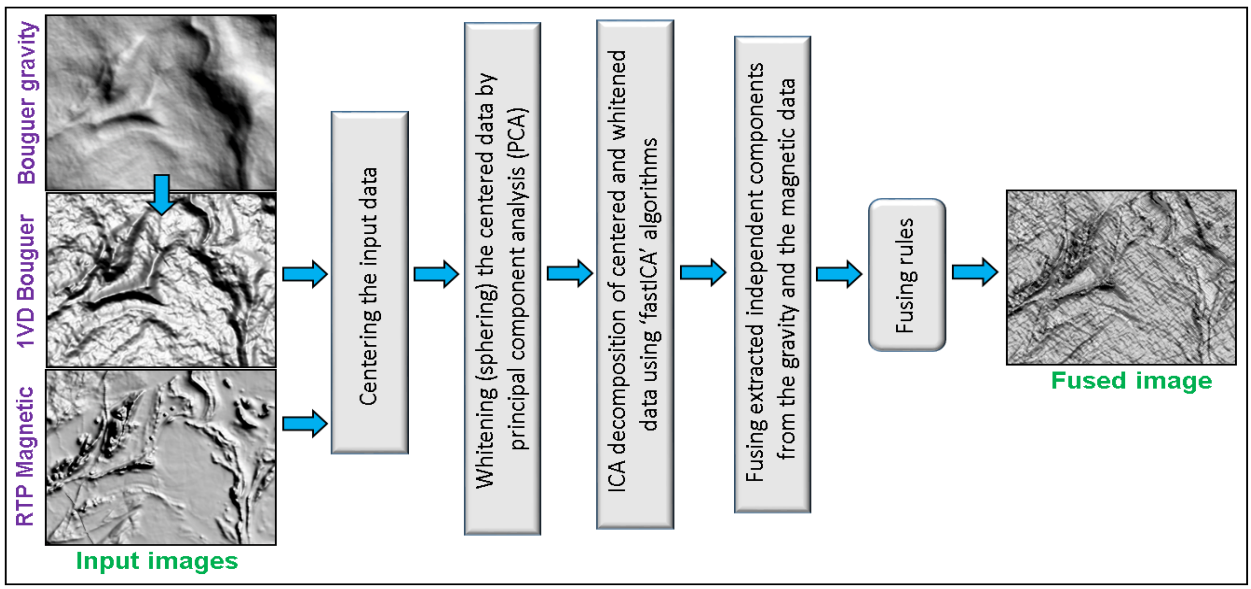

Figure 3. The workflow of the ICA fusion technique used in this study.

Prior to applying the ICA-based fusion to the data, both the first vertical derivative of the Bouguer gravity anomaly and the reduced to the pole total magnetic intensity images were subjected to two statistical transforms; centering and whitening (Fig. 3). These two statistical transforms are necessary in order to run ICA correctly. Centering transform was accomplished by subtracting the value of each pixel in the gravity and the magnetic images from their corresponding mean values (DC offset), in order to make the new mean values of the gravity and the magnetic images equal to zero. Whitening (aka, sphering) transform was performed in order to remove any correlations that may exist in the gravity and the magnetic images. This transform was carried out by applying principal component analysis (PCA) to the centered gravity and magnetic images.

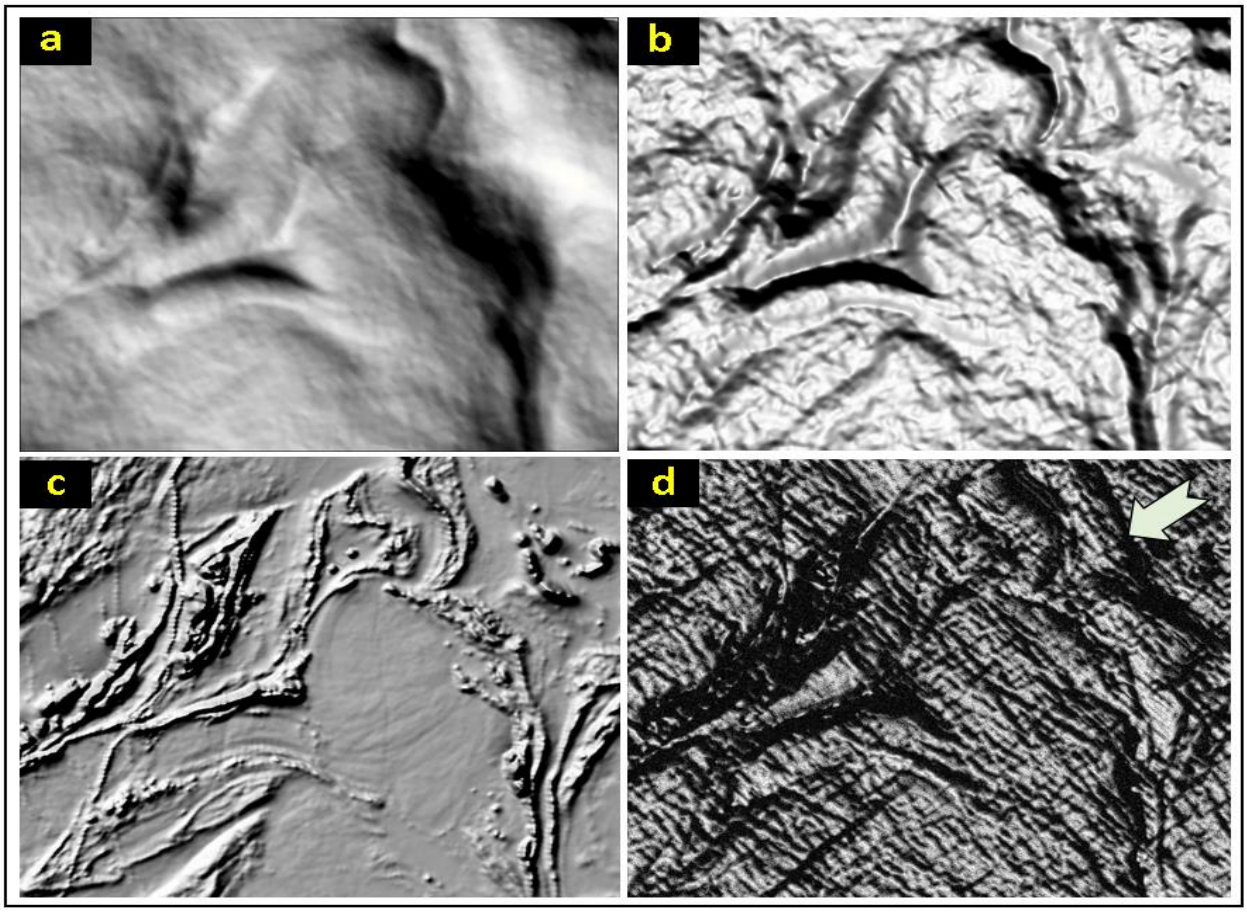

Figure 4. Gravity and magnetic images used in this study: (a) Bouguer gravity; (b) First derivative of Bouguer gravity; (c) reduced-to-pole total magnetic field; (d) fused gravity and magnetic image.

Results

The final ICA-based fused image obtained from fusing the first vertical derivative of the Bouguer gravity anomaly image (Figure 4b) and the reduced to the pole total magnetic intensity image (Fig. 4c) is shown in Figure 4d. In comparison to the original gravity and magnetic images, the

fused image in Figure 4d highlights a number of significant geological features that are not well-defined on the individual gravity and magnetic images, for example, the NNW-trending structure in the NE corner of the area. The fused image also reveals a number of distinct linear and curvilinear features that are mainly trending in the WNW-ESE and SW-NE directions. These linear and curvilinear features are most likely related to folds, faults and fractures in the Precambrian basement rocks and their overlying sedimentary and meta-sedimentary rocks.

Conclusions

In this study, we applied a fusion technique based on a powerful machine learning statistical technique known as independent component analysis (ICA) to fuse gravity and magnetic images. The gravity and the magnetic data were acquired at the same time and from the same airborne gravity gradiometry survey that was flown over the McFaulds Lake area in Ontario, Canada. The aim was to extract the most important and statistically independent geological features from the gravity and the magnetic images and fuse them into a single fused image. The integrated information in the fused image provide a more objective and a more efficient way to analyze and interpret the data. The fused image obtained in this study reveal a number of well-defined linear and curvilinear geological features that are not obvious on the individual gravity and magnetic images. We believe that these linear and curvilinear features are most likely represent footprints of folds, faults and fractures that are intersecting the Precambrian basement rocks and their overlying sedimentary and meta-sedimentary rocks.

References

Chandler, V. W., J. S. Koski, W. J. Hinze, and L. W. Braile, Analysis of multisource gravity and magnetic anomaly data sets by moving-window application of Poisson's Theorem, *Geophysics*, **46**, 30–39, 1981.

Cranston, D., 2010, "Ring of Fire" investment opportunities in Ontario's far North; Ontario Ministry of Northern Development Mines and Forestry, 25p.

Dyer, R.D., and Burke, H.E, 2012, Preliminary results from the McFaulds Lake ("Ring of Fire") area lake sediment geochemistry pilot study, northern Ontario; Ontario Geological Survey, Open File Report 6269, 26p.

Goussev, S.A., Hassan, H.H., Shield, G.W. and Cokinos, J.S., 2009, Fusion of enhanced gravity and magnetic signatures for continental-oceanic boundary (COB) mapping: offshore Gabon example; SEG Convention, Workshop Poster, Houston.

Hassan, H. H. and Peirce, J. W., 2008, Fusion of airborne gravity and magnetic images for improved detection of structural control; 2008 CSPG-CSEG-CWLS Convention, Calgary, Alberta, 4p.

Hyvärinen, A., 2013, Independent component analysis: recent advances; Philosophical Transactions of the Royal Society of London, A371, 20, 110-534.

Ontario Geological Survey and Geological Survey of Canada, 2011, Ontario airborne geophysical surveys, gravity gradiometry and magnetic data, grid and profile data (ASCII and Geosoft formats) and vector data, McFaulds Lake area; Ontario Geological Survey, Geophysical Data Set 1068.